Prediction of solute diffusivity in Al assisted by first principles molecular dynamics

O. M. Løvvik[1], E. Sagvolden[1], Y. J. Li[2]

[1]SINTEF Materials and Chemistry, P.B. 124 Blindern, 0314 Oslo, Norway

[2]SINTEF Materials and Chemistry, P.B. 4760 Sluppen, 7465 Trondheim, Norway

Abstract

Ab initio calculations of the solid-state diffusivity of solute atoms in bulk aluminium have previously been based on transition-state theory (TST), employing systematic assessments of single jumps, and transition-state searches and using an approximate model of jump frequencies and correlation factors like the five-frequency model. The present work compared TST benchmark predictions of diffusivities with first-principles molecular dynamics (FPMD). The TST calculations were performed at unprecedented high precision, including the temperature-dependent entropy of vacancy formation which has not been included in previous studies of diffusion in Al; this led to improved agreement with experimental data. It was furthermore demonstrated that FPMD can yield sufficient statistics to predict the frequency of single jumps, and FPMD was used to successfully predict the macroscopic diffusivity of Si in Al. The latter is not possible in systems with higher activation energies, but it was demonstrated that FPMD in such cases can identify which jumps are prevalent for a given defect configuration. Thus, information from FPMD can be used to simplify the calculation of correlation terms, prefactors and effective transition barriers with TST significantly. This can be particularly important for the study of more complicated defect configurations, where the number of distinct jumps rapidly increases to be intractable by systematic methods.

1 Introduction

Diffusion is a controlling process for many metallurgical reactions, in particular during heat treatment of alloys. In-depth understanding of the diffusion mechanism of different alloying elements and precise experimental measurement/calculation of their diffusion constants are critical for development of reliable microstructure simulation models of alloys.

Modelling of diffusion of impurity elements in Al alloys has until quite recently been performed using empirical or semi-empirical approaches.[1, 2] This can give good correspondence with experimental data, but the transferability to other systems and predictive power of such methods are limited. However, increased computational power and development of efficient methods have made calculations from first principles (FP) on such systems feasible. While this has usually relied on experimental input for some of the parameters,[3-7] it is possible to calculate the diffusion coefficients entirely from first principles, with excellent correspondence with experimental data.[8, 9] This approach entails the hopping frequency calculated with transition state theory (TST),[10] computing the rate of hopping from the energy of transition states and vibration frequencies. This is combined with a correlation factor incorporating the conditional probability of the direction of a hop given the direction of the last hop. The transition state is typically computed with the nudged elastic band method (NEB),[11] in which the saddle point is located by minimizing the energy perpendicular to the transition path, while at the same time maximizing it along the transition path. The transition barriers of single solute atoms in face-centered cubic (fcc) Al were calculated by Simonovic *et al*. within this scheme, using a simplified version of the five-frequency model; they calculated all relevant transition barriers, but picked out only the lowest

ones as the rate-limiting step in the diffusion process.[9] This simplified the calculations significantly, and they were thus able to calculate effective diffusivities for a large range of solute elements, including all transition metals.

When such a task has been finished, there is an urge to move further to more complicated systems like multiple component alloys with more than one solute. A main challenge with the approach above is then that one needs to compute the transition states, their energies and vibrational spectra for all relevant inequivalent types of jumps. The complexity of this assignment rapidly increases with the dimensionality, and there is no available technique similar to the five-frequency model even for the ternary system, containing two different solutes. As the symmetry decreases further, the ensemble of possible transition states can grow to sizes which are not easily accessible with traditional methods.

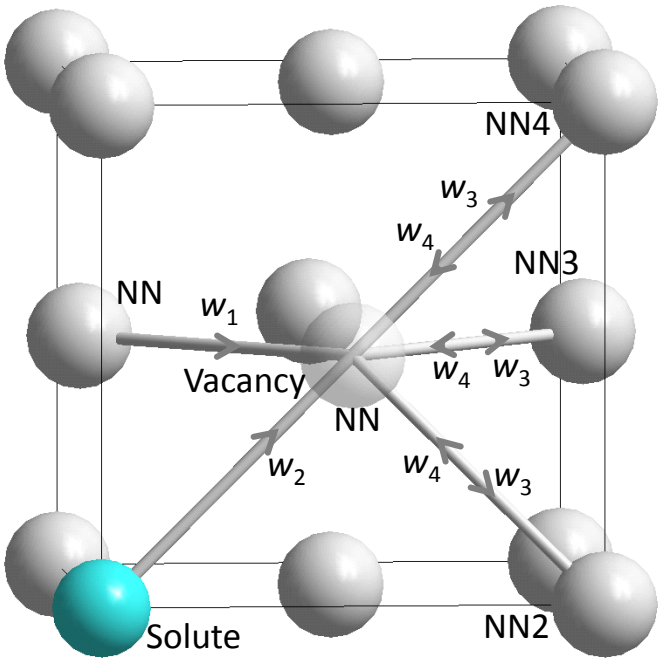

Figure 1. The surroundings of a vacancy and a nearby solute atom. Here the vacancy is shown at a nearest neighbour position (NN) to the solute. Also illustrated are representative second (NN2), third (NN3) and fourth (NN4) nearest neighbours.

One alternative path to map out all the possible diffusion routes within a complicated system is kinetic Monte Carlo (KMC), creating a library of jump rates for inequivalent jumps and propagating the system randomly based on these rates.[12, 13] This has many advantages; it can in principle be upscaled to macroscopic scales, and it can easily handle rare events since the barriers are calculated.

In the present work, we have chosen a somewhat different approach: first-principles molecular dynamics (FPMD) simulations for direct prediction of the diffusivities. This requires no information about different inequivalent jumps, and has the potential to be much less labour-intensive than a systematic approach for complicated defect structures. It will also work in systems without well-defined sites, like in amorphous materials.[14] We have investigated whether such a parameter-free and automatic technique based on DFT can be used to assess the diffusivity of solutes in Al. If successful, this can give access to much more complicated systems without the need to define and quantify a large set of possible transition states. It can even give valuable

information about systems where there are no well-defined transition states, or where they change with time. A further advantage is the correct identification of unintuitive, yet actual, configurations, which may be missed by other techniques.

The main challenge with FPMD is to obtain sufficient statistics. Long simulation times may be needed to achieve adequate data for accurate predictions of diffusivities. In order to capture the diffusion of a solute with a reasonable accuracy, it is necessary to obtain at least a handful of the most relevant jumps within the simulation timescale, which presently is limited to 10-100 ps, depending on the system size and available computational resources. (One simulation time step is typically in the order of 1 fs, which requires a computational resource of at least 100 CPU seconds if the present system is to be calculated self-consistently within DFT using contemporary supercomputing resources.) A typical trial frequency of a jump is ~10 THz, and we would need jump frequencies at least in the order of 0.1 THz to obtain some statistics of jumps. If the simulation temperature is restricted by the melting temperature of Al (933 K) and by a reasonable number of simulation steps (say, $\sim 10^6$ steps of 1 fs each, costing $\sim 10^4$ CPU seconds), the highest transition barrier which can be described by DFT (that is, with at least a few jumps in average per simulation) is ~75 kJ/mol. The activation energies for solute diffusion in Al are between 100 and 250 kJ/mol (representing a large number of solutes),[9] and the corresponding transition barriers are between 40 and 200 kJ/mol. This means that some but not all jumps will be available by FPMD with the restrictions above. For the highest barrier of 200 kJ/mol, the average simulation time between each diffusive jump would cost $\sim 10^{11}$ CPU hours by using state-of-the-art DFT based MD.

It is fortunately possible to run simulations at higher temperatures without melting within the relevant time spans. As we will see later in this paper, simulations can be performed in Al at temperatures up to 1800 K without the structure melting during the time scale of the simulation. A superheated temperature of 1800 K gives access to transition barriers up to ~140 kJ/mol given the restrictions mentioned above. This is still not enough to describe the complete diffusion process; the CPU cost of an average diffusive jump with a transition barrier of 200 kJ/mol would be $\sim 10^6$ hours. Also, it is very likely that the structure will melt during such time spans.

Nevertheless, this illustrates that single jumps with low barriers should be accessible through simulations lasting for several ps. The cost of such simulations would be some thousands of CPU hours, which is clearly within reach with current massively parallel supercomputers. Thus, there is a good prospect of using first-principles based MD for qualitative assessments of the relative abundance of different jumps. In some lucky cases, one can also anticipate quantitative results from such simulations.

We have in the present paper compared the usefulness of transition state theory and FPMD for calculating solute diffusivities. In particular, we have focused on the possibility of using FPMD to simplify the systematic calculations of jump frequencies and correlation factors within the TST framework. In order to have a proper benchmark system we have also performed TST calculations of high precision.

2 Methodology

We assessed the diffusivity of Mn, Si and Fe in Al using transition state theory (TST) and first-principles molecular dynamics (FPMD). Both techniques were based on density functional theory (DFT), using the Vienna *ab initio* simulation package (VASP).[15, 16] We used the local density approximation (LDA),[17, 18] since this has been shown to give best correspondence with experimental data.[8] This is probably caused by the better surface energies provided by LDA (because of fortuitous cancellations of errors), which gives better vacancy energies.

Transition state theory within the five-frequency model was employed in a similar manner as in Refs. 8, 9. This takes into account the probability of various jumps in the vicinity of a solute atom, as shown in Figure 1. The jump frequencies of the different kinds of jumps are here marked by w_n. The diffusion is vacancy mediated, and the rate limiting step is either by the vacancy and solute interchanging places ("solute jumps") or by the vacancy and a neighbour Al interchanging places. Thus, the model can be formulated as follows:

$$D = f_2 w_2 a^2 \exp\left(-\left(G_{vac} - G_{dissoc}\right)/kT\right) \qquad \textbf{(1)}$$

The diffusivity D depends on a correlation factor f_2, the frequency of solute jumps w_2, the jump length a, the free energy of vacancy formation G_{vac}, the free energy of vacancy-solute dissociation G_{dissoc}, and the temperature T. k is the Boltzmann constant. The jump frequencies were calculated using DFT from the following formula [10]:

$$w = \nu^* \exp\left(\frac{-\Delta H_m}{k_B T}\right). \qquad (2)$$

The effective frequency ν^* is the product of the vibrational frequencies of the initial state divided by those of the transition state. This was obtained from the Hessian matrix using density functional perturbation theory. The jump barrier ΔH_m is the change in enthalpy of the system between the initial state and the transition state; in practice this is the difference in calculated total electronic energy between the two states calculated by DFT with the nudged elastic band (NEB) formalism.

Calculation of f_2 was done according to Eq. 2 in Ref. 8, requiring jump frequencies of the dissociation step w_3. As can be seen in Figure 1, there are three such steps (from NN to NN2, NN3, or NN4). We calculated all these possibilities, and report here the ones with highest frequency at 400 K; usually this was the one with lowest transition barrier. The barrier between the three w_3 options differed by up to 16 kJ/mol, and the jumps to NN3 and NN4 always exhibited smaller barriers than jumps to NN2.

All DFT calculations used a super cell consisting of 3x3x3 cubic conventional cells containing 106 Al atoms, one vacancy and one solute atom. This prevented artificial interactions between periodic images of the defects. The Al lattice constant was always kept at the LDA relaxed value of 0.399 nm. The solute atom was Si, Fe or Mn. The TST calculations were performed at two different levels of accuracy, in order to compare directly to previously published data and to the FPMD simulations which were performed at rather low accuracy. The high-accuracy calculations employed a plane wave cutoff of 350 eV and a **k** point density of 7x7x7, corresponding to a distance between **k** points of 0.012 Å^{-1} in each direction. The **k** point density is the most critical parameter for achieving numerical convergence in this system, and reducing the sampling to 5x5x5 (**k** point distance of 0.017 Å^{-1}) introduced large errors for some configurations – e.g. for Mn-vacancy exchange, the barrier changed by 36 kJ/mol when increasing the **k** point density from 5x5x5 to 7x7x7. Increasing the density further is not necessary; the high-accuracy computations using 7x7x7 **k** points reproduced 9x9x9 **k**-point barriers for Mn-vacancy exchange to within 0.3% (less than 1 kJ/mol). This was hence postulated to be a sufficiently accurate benchmark level. Spin polarization was included in cells with odd numbers of electrons, since this has previously been demonstrated to be important.[9] The low-accuracy calculations used similar numerical parameters as those described below for the MD simulations.

The FPMD simulations were performed with 1 fs time steps for 25 ps. The vacancy and solute started as nearest neighbours. Temperatures were fixed with a micro canonical ensemble at temperatures in steps of 100 K from 900 K to 2000 K (12 simulations). Computations were performed using the gamma point only for the **k** point sampling. The plane wave energy cutoff

was 184.3 eV for Si, 201.0 eV for Fe and 202.5 eV for Mn diffusion in Al. All FPMD calculations were performed without allowing spin polarization.

We tracked the vacancy during the FPMD run, and all single jumps of the vacancy were identified. Furthermore, the time spent by the vacancy at the various sites (nearest neighbour of the solute NN1, NN2, etc.) was quantified. The jump frequency was then calculated simply as the number of jumps divided by the total dwelling time at the initial site of the jump. The advantage of this method is that the anisotropic site occupancy (the initial state of the vacancy was always the NN1 site) will be cancelled out when dividing with the dwelling time.

3 Results and discussion

3.1 Transition state theory

First the enthalpy of formation of the solute, the vacancy, the solute-vacancy binding energy and the difference energy between solutes and vacancies being nearest neighbours and *n*'th nearest neighbours were calculated. They are defined as follows:

$$\Delta H_{\text{sol}} = E(\text{Al}_{N-1}X) - (N-1)E(\text{Al}) - E(X),$$

$$\Delta H_{\text{vac}} = E(\text{Al}_{N-1}\text{Vac}) - (N-1)E(\text{Al}),$$

$$\Delta E_{\text{NN}n} = E(\text{Al}_{N-2}X\text{Vac; NN1}) - E(\text{Al}_{N-2}X\text{Vac; NN}n),$$

$$E_{\text{sol-vac}} = E(\text{Al}_{N-2}X\text{Vac; NN1}) + NE(Al) - E(\text{Al}_{N-1}X) - E(\text{Al}_{N-1}\text{Vac}),$$

where E is the total electronic energy as calculated by VASP, X is the solute, and Vac is the vacancy. A configuration where the solute and vacancy are *n*'th nearest neighbours is designated by NN*n*. The results are shown in

Table 1, with the enthalpies and energies given in kJ/mol.

Table 1. The enthalpy of formation of a vacancy ΔH_{vac}, a solute ΔH_{sol}, and the interaction energy between the solute and the vacancy $E_{sol\text{-}vac}$ calculated by DFT, as defined in the text. Also shown is the calculated energy difference between the solute and vacancy being nearest neighbours and *n*'th nearest neighbours ΔE_{NNn}. All enthalpies and energies are given in kJ/mol. The calculations were performed at high level of precision for benchmarking . The results have been compared to previous calculations and experiments.

Solute	Enthalpies (kJ/mol)	This work	Previous calculations	Expt.
Al	ΔH_{vac}	67	72[a], 69[b]	65[c]
Si	ΔH_{sol}	31		
	ΔE_{NN2}	-6		
	ΔE_{NN3}	-4		
	ΔE_{NN4}	-6		
	$E_{sol\text{-}vac}$	-4	5[a], 11[b]	3[d]
Mn	ΔH_{sol}	-26		
	ΔE_{NN2}	9		
	ΔE_{NN3}	6		
	ΔE_{NN4}	12		
	$E_{sol\text{-}vac}$	8	-6[a]	
Fe	ΔH_{sol}	-51		
	ΔE_{NN2}	1		
	ΔE_{NN3}	-1		
	ΔE_{NN4}	2		
	$E_{sol\text{-}vac}$	2	-2[a]	

[a] Ref. 9

[b] Ref. 8

[c] Ref. 19

[d] Ref. 20

We first note that the calculated values in the present work are comparable to previously published studies (see Ref. 21 and references therein.) The enthalpy of formation for solutes is negative for Mn and Fe, but this is a result of the choice of the pure elements in their standard state for the reference energies. This would change if we e.g. also took into account the possibility of oxide formation. The solute-vacancy interaction is slightly attractive for Si, while it is clearly repulsive for Mn. In the case of Fe, the interaction energy is so low that no effective repulsion or attraction can be inferred. Since adjacent vacancies are necessary for solute diffusion to take place, this will contribute to decreasing the diffusivity of Mn in Al, since the solute-vacancy repulsion will lead to a small number of solute-vacancy pairs. The relatively small discrepancy with previous calculations may be ascribed to different level of theory (Ref. 8 modified their LDA results with a surface energy correction, while Ref. 9 used GGA.)

To elucidate how the vacancy may dissociate from the solutes we have also computed total energies of the solute-vacancy pair with varying distances. This is shown in

Table 1 as the energy difference between having the vacancy as the n'th nearest neighbour of the solute NNn and having it as the nearest neighbour NN1. The interaction energy $E_{\text{sol-vac}}$ then corresponds to $\Delta E_{\text{NN}n}$ when n is very large. The calculations were performed at the higher level of accuracy described in the methods section. As we can see, the energy profile is relatively flat; in no case is the energy difference greater than 12 kJ/mol. We also see that the interaction between the solute and vacancy does not change monotonously as their distance increases; in the case of Fe there is e.g. a weak attractive force between the solute and vacancy when they are third-nearest neighbours (NN3), while it is repulsive at all other calculated distances.

The jump barriers and frequencies of the various jumps shown in Figure 1 were then calculated and represented on the form defined in Eq. (2). The jump barriers ΔH_m are presented in

Table 2 and the prefactors ν^* in

Table 3. We first note that the calculated jump barriers ΔH_m are not very sensitive to the level of accuracy – the very cheap calculations with low precision differ by less than 20% or 20 kJ/mol from those of the benchmark level, which means that the low level calculation can be used with enough confidence to distinguish high barriers from low ones. The low level calculations could thus in all cases identify the rate-limiting step.

When we compare our calculations to previous ones using comparable techniques, there are significant differences. Our calculated transition barriers are consistently around 20% higher than those of Ref. 9, most probably due to the use of LDA in the present study and GGA in Ref. 9. A notable exception is the diffusion of Mn, where our predicted E_b of w_2 is 184 kJ/mol, compared to 90 kJ/mol in Ref. 9. It is difficult to explain why this is so, even after performing thorough tests of various accuracy parameters. Adding spin polarization did not change our result by far as much as in Ref. 9.

The frequencies ν^* listed in

Table 3 are very sensitive to the precision. They are clearly unreliable when calculated by TST at the low precision level, in some cases differing by several orders of magnitude from those calculated at high numeric precision. This reflects the high sensitivity of frequencies with respect to energies; small errors in energies can result in large errors in frequencies, since the latter are calculated from rather small energy changes to ensure that the potential energy is in the harmonic region. The frequencies have therefore not been reported at the low precision level from TST in

Table 3.

Table 2. DFT calculated energy barriers ΔH_m in kJ/mol of the single jumps defined in Figure 1; w_0 (Self-diffusion), w_1 (NN1-NN1 rotation), w_2 (Solute-vacancy exchange), w_3 (NN1-NN*n* dissociation), w_4 (NN1-NN*n* association). The numbers have been obtained with first-principles molecular dynamics (FPMD) simulations and transition state theory (TST) at two levels of precision; the same low level as the FPMD calculations, and a higher level. Refer to the Methodology section for details. The results are compared to previous publications.

Solute	Jump	FPMD	TST (Low prec.)	TST (High prec.)	TST (previous calcs.)
Al	w_0	47	50	60	49[a], 56[b]
Si	w_1	47	42	52	46[a], 50[b]
	w_2	41	47	53	44[a], 53[b]
	w_3	55	50	60	54[a], 64[b]
	w_4		45	55	53[b]
Mn	w_1		19	23	
	w_2		203	184	90[a]
	w_3	71	60	62	
	w_4		61	68	
Fe	w_1	40	17	22	
	w_2		188	167	131[a]
	w_3	67	60	62	
	w_4		53	61	

[a] Ref. 9

[b] Ref. 8

Table 3. DFT calculated prefactors ν^* in THz of the single jumps defined in Figure 1; w_0 (Self-diffusion), w_1 (NN1-NN1 rotation), w_2 (Solute-vacancy exchange), w_3 (NN1-NN*n* dissociation), w_4 (NN1-NN*n* association). The numbers have been obtained with first-principles molecular dynamics (FPMD) simulations and transition state theory (TST) at two levels of precision; the same low level as the FPMD calculations, and a higher level. Refer to the Methodology section for details. The results are compared to previous publications.

Solute	Jump	FPMD	TST (High prec.)	TST (previous calcs.)
Al	w_0	38	6	17[a]
Si	w_1	16	5	11[a]
	w_2	5	4	16[a]
	w_3	49	6	22[a]
	w_4		5	14[a]
Mn	w_1		2	
	w_2		19	
	w_3	167	5	
	w_4		11	
Fe	w_1	40	2	
	w_2		[b]	
	w_3	55	6	
	w_4		9	

[a] Ref. 8

[b] This jump exhibited non-harmonic behaviour at the transition state, so the prefactor was undefined. See the text for details.

One of the jump prefactors could not be calculated with density functional perturbation theory; the solute-vacancy exchange w_2 of Fe in Al. In this case the frequency of the phonon mode perpendicular to the transition path was very small, and a reliable number for the prefactor could not be obtained. The reason was most likely that the magnitude of this frequency was similar to that of the numerical uncertainty due to limited **k** point density. This is thus not reported in Table 3. When calculating the total diffusivity below, we have estimated the Fe diffusivity by roughly allocating the value 10 THz to w_2. This is probably too low (since the transition state is broad perpendicular to the jump direction), but it gives an estimate of the order of magnitude. This problem was not detected at lower precision (less **k** points); the frequency was then calculated to be significantly larger (but strongly dependent on the **k** point density), which may explain why this has not been reported previously.

The resulting overall diffusivity D generally exhibits Arrhenius behaviour:

$$D = D_0 \exp\left(\frac{-Q}{k_B T}\right). \qquad (3)$$

The activation energy Q is given by[8]

$$Q = \Delta H_{\mathrm{m}} + \Delta H_{vac} - E_{\text{sol-vac}} - k_B T_f \,, \quad (4)$$

where

$$T_f = \frac{d(\ln f_2)}{d(1/T)}. \qquad (5)$$

The contribution from $k_B T_f$ is temperature dependent, and the values for Q in Table 4 have been calculated at $T = 400$ K. For Si diffusion, the value of $k_B T_f$ increases from 0.2 to 0.9 kJ/mol when T increases from 400 to 1000 K, while it is less than 10^{-5} kJ/mol even at 1000 K for Mn and Fe diffusion.

The prefactor D_0 can be written as[8]

$$D_0 = \frac{f_2 a^2 \nu^* \exp\left(\frac{\Delta S_f}{k_B}\right)}{\exp\left(\frac{k_B T_f}{k_B T}\right)} \qquad (6)$$

The denominator of this expression is very close to 1 for all relevant temperatures, and has therefore been neglected. The correlation factor f_2 was calculated to be almost identical to 1 for Mn and Fe. For Si, it varied from 0.64 at 400 K (which was used in the following calculations) to 0.75 at 1700 K. The entropy of vacancy formation is in the supercell approach given by[4]

$$\Delta S_f = S_{vac} - \frac{N-2}{N-1} S_{perf}, \qquad (7)$$

where S_{vac} and S_{perf} are the vibrational entropy of the supercell with a vacancy and the perfect lattice, respectively. N is the number of atoms in the perfect supercell (108 in our case), and the term (N–2/N–1) follows from the number of degrees of freedom, which is ($3N - 3$) for the perfect and ($3(N - 1) - 3$) for the cell with vacancy. Each of these entropies are given as

$$S = k_B \sum_i \left(\frac{h\nu_i}{k_B T\left[\exp\left(h\nu_i / k_B T\right) - 1\right]} - \ln\left[1 - \exp\left(h\nu_i / k_B T\right)\right] \right). \qquad (8)$$

The sum runs over all phonon frequencies ν_i. This means that ΔS_f is temperature dependent; a plot of this is displayed in Figure 2. It stabilizes around 2.5 k_B above 300 K, and we have used the value at 400 K to calculate D_0: $\Delta S_f(T = 400\ \mathrm{K}) = 2.51\ k_B$, and $\exp\left(\frac{\Delta S_f}{k_B}\right) = 12.3$. These results are very similar to those obtained for Li.[4]

In the high-temperature limit the entropy can be approximated as $S = k_B \sum_i \left(1 - \ln\left[\exp\left(h\nu_i / k_B T\right)\right]\right)$,[22] and the contribution to D_0 from ΔS_f then becomes

$$\exp\left(\frac{\Delta S_f}{k_B}\right) = \frac{\left(\prod_{i=1}^{3N-3} \nu_i^p\right)^{\frac{N-2}{N-1}}}{\left(\prod_{i=1}^{3N-6} \nu_i^v\right)}, \qquad (9)$$

where ν_i^p and ν_i^v are the phonon frequencies of the perfect lattice and lattice with vacancy, respectively. In this limit, we get that $\Delta S_f(T \to \infty) = 2.60\ k_B$, and $\exp\left(\frac{\Delta S_f}{k_B}\right) = 13.5$. Note that this value is quite different from that of previous studies.[23, 24] With our more detailed methodology, higher **k** point density and larger unit cell, we were unable to confirm the previously published values for ΔS_f.

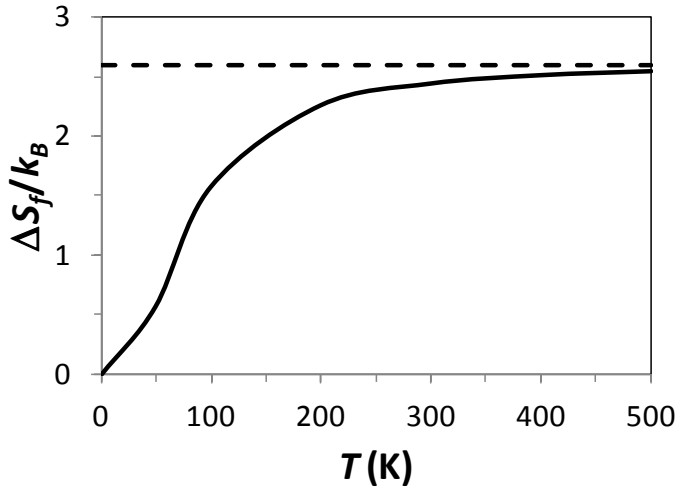

Figure 2. The entropy of vacancy formation ΔS_f as function of temperature, calculated according to Eq. 7 and 8. k_B is Boltzmann's constant. The value at 400 K (2.51 k_B) was used for calculating the prefactor D_0 in Eq. 6. The dashed line designates the high-temperature limit corresponding to Eq. 9.

The TST-calculated activation energies are shown in

Table 4. We first note that they are quite similar to those calculated in previous studies, as well as those found in experimental studies. Diffusion of Mn is again an exception, originating from the large difference in w_2 discussed above. The experimental value of Q in Mn (211.5 kJ/mol) is in between the values calculated in the literature (between 168 and 269 kJ/mol), and can thus not be used to distinguish between the results.

Turning to the TST-calculated prefactors D_0 which are shown in Table 5, we see that our TST-calculated values are also in quite good correspondence with previous studies. This is despite the very high sensitivity of calculated frequencies on the accuracy and methodology. Choosing LDA or GGA can influence this significantly, as can changing the **k** point density, force relaxation criterion or other numerical parameters. Thus, the numbers are reliable only within an order of magnitude or so. Our results differ significantly from the experimental values presented in Table 5, particularly in the case of Mn and Fe. One reason may be the abovementioned uncertainties of our calculations, or that our idealized unit cell does not represent the system properly. But the measurements may also involve large uncertainties. As an example, literature data on Fe diffusion in Si contain prefactors from 5E-03 to 90 m^2/s,[25-29] a spread of more than 4 orders of magnitude. This still indicates that our values are too low compared to experimental data. It is difficult to identify the reasons for such a large discrepancy with certainty.

Table 4. The activation energy *Q* in kJ/mol of Al self-diffusion and Si, Mn, and Fe diffusion in Al is given, calculated by DFT according to Eq. 4. Two levels of theory are reported: DFT based molecular dynamics (FPMD) and TST at high accuracy (Hi-TST). The results are compared to previous calculations and experiments. Reference 25 is a critical review of several experimental studies, and the numbers presented in this table represent the best fit.

Solute	FPMD (this work)	TST (High prec., this work)	TST, previous calcs.	Expt.
Al	115	117	121[a]	120.6[d]
Si	119	124	111[a], 113[b], 98[c]	117.6[e]
Mn		243	168[b], 171[c], 269[f]	211.5[e]
Fe		233	205[b], 206[c], 246[f]	214.0[e]

[a] Ref. 8

[b] Ref. 9

[c] Ref. 30

[d] Ref. 31

[e] Ref. 25

[f] Ref. 32

Table 5. The diffusivity prefactor D_0 in m^2/s of Al self-diffusion and Si, Mn, and Fe diffusion in Al is given, calculated by DFT according to Eq. 6. Two levels of theory are reported: DFT based molecular dynamics (FPMD) and TST at high accuracy (Hi-TST). The results are compared to previous calculations and experiments. Reference 25 is a critical review of several experimental studies, and the numbers presented in this table represent the best fit.

Solute	FPMD	TST (High prec.)	TST, previous calcs.	Expt.
Al	3.0E-06	6.1E-06	7.0E-06[a]	1.10E-05[c]
Si	3.9E-07	2.7E-06	3.7E-06[b]	1.38E-05[d]
Mn		1.9E-05	2E-05[e]	1.35E-02[d]
Fe		1.E-05[f]	3E-05[e]	3.62E-01[d]

[a] Ref. 8

[b] Ref. 9

[c] Ref. 31

[d] Ref. 25

[e] Ref. 32

[f] This is only an estimate of the order of magnitude, assuming that $\nu^* = 10$ THz for w_2. See the text for details.

3.2 First-principles molecular dynamics

All temperatures used in the FPMD runs were above the melting point of Al which is 933.47 K. The high temperatures were chosen in order to increase the frequency of jumps, to improve statistics from 25 ps MD runs. However, if the system were to actually behave as molten, one

would get molten diffusion. Then, the diffusion mechanism is qualitatively different from that of vacancy mediated diffusion, and the diffusion data hence found would be irrelevant. Yet, even though the temperatures are higher than the melting point, the system does not necessarily melt. It is well-known that significant over-heating (that is, heating above the melting point without melting) can occur during MD simulations lasting for several picoseconds when using crystalline models like the ones studied here.

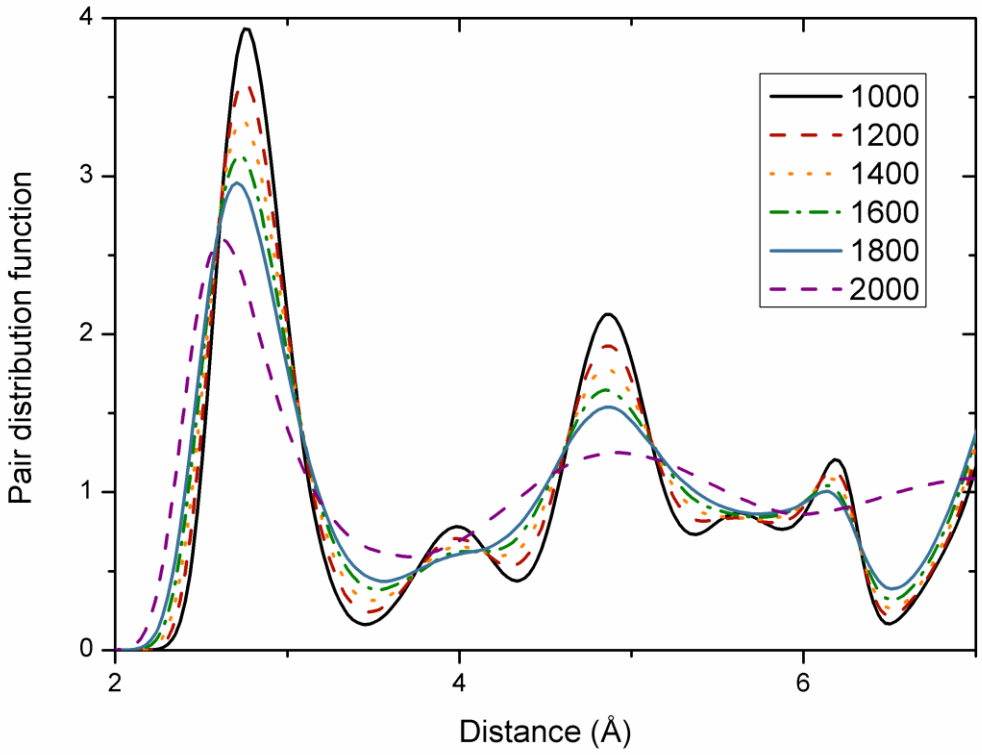

Figure 3. The pair distribution function (PDF) at different temperatures in K for Si diffusion in Al. The PDF is calculated for an ensemble of 15000 time steps at the specified temperature, after an initial equilibration of 10000 time steps. Each time step is 1 fs. The melting point of our simulation is between 1800 K and 2000 K. Staying at or below 1800 K should therefore give vacancy mediated diffusion.

To determine whether the system has melted, we used the pair distribution function, which gives the probability of finding an atom at a given distance from another atom. In a crystal at T=0 K, the pair correlation function will consist of high and sharp peaks. As the temperature increases, thermal vibration will smear the peaks out, but they will still be well-defined. That changes when the sample melts. There will be no long-range ordering in the sample and therefore most of the peaks will be smeared out. In Figure 3, we display the pair correlation function for the $Al_{106}Si$ system at temperatures from 1000 K to 2000 K. We see that there is a dramatic change in the smearing when going from 1800 K to 2000 K, indicating that this is the point where the sample melts (at our level of theory and constraints, as discussed above). Therefore, as long as we keep ourselves at or below 1800 K, the diffusion mechanism should be the same as at lower temperatures. Going above this "melting point" however, we risk studying molten diffusion instead.

The results for Si diffusion are shown in Figure 4. They are based on around 320 distinctive jumps distributed among 10 simulations at different temperatures. The total simulation time for all the simulations was 250 ps. The most common jump was self-diffusion of Al (after complete dissociation of the solute-vacancy pair) with around 100 jumps. The solute-vacancy exchange only happened three times, at three different temperatures. We see that almost all the jumps have relatively well-defined exponential fitting curves, which have been used to calculate the prefactor and transition barrier for each jump. The exception is the jump back to NN1 (restoration of the solute-vacancy pair), which has too large spread in the values for the fit to be well-defined. The R^2 value for this fit was 0.0006. Also note that even if the solute-vacancy exchange is very well-behaving (with $R^2 = 0.93$), this is rather fortunate. With only three jumps contributing to the plot, small changes in e.g. one of the dwelling times could have changed the situation considerably.

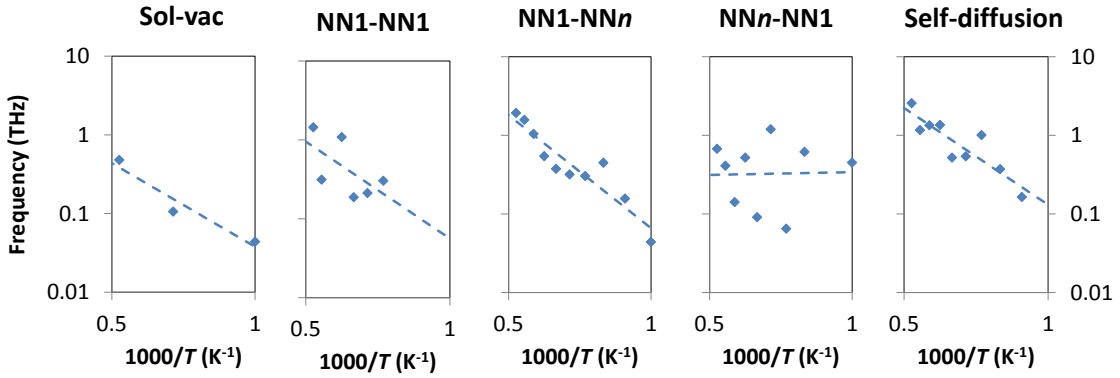

Figure 4. Arrhenius plots of the calculated frequencies as a function of temperature for different atomic jumps in the FPMD simulations with a Si solute. The jumps are, from left to right: exchange of the solute and vacancy (w_2, "Sol-vac"), nearest neighbours rotating around the solute (w_1, NN1-NN1), dissociation of the solute-vacancy pair (w_3, jump of the vacancy from NN1 to any of NN2, NN3, or NN4), reestablishment of the solute-vacancy pair (w_4, jump of the vacancy from any of NN2, NN3, or NN4 to NN1), and self-diffusion of Al when the vacancy is located further away from the solute than NN4 (w_0). Fitting of the data to exponential functions is shown by the dashed curves.

Nevertheless, the FPMD results of Si diffusion gave four temperature dependent jump frequencies, all displaying both a prefactor and a transition barrier. They are presented in

Table 2 and

Table 3 and compared to similar numbers from transition state theory, both made in this and other studies.[8, 9] It is encouraging to see that all the energies calculated by FPMD are within a few percent away from those from TST. Most of the frequencies are also in fair agreement with the TST results. This is very promising, given the notorious difficulty of calculating and measuring such frequencies with high precision. The diffusivity of Si in Al, presented in

Table 4, is also in very good correspondence with our TST calculations as well as previous calculations and experimental results.

FPMD simulations using the other solutes gave less valuable outcomes. In the case of Mn, only the dissociation jump (NN1-NN*n*) gave good enough statistics to calculate an energy barrier with prefactor for w_3 from an Arrhenius plot fit like those in Figure 4. This reflects the repulsive interaction between Mn and the vacancy, and means that neither w_1 nor w_2 were available from FPMD. However, this does not mean that the results are useless. The rapid dissociation of the solute-vacancy pair means that the solute-vacancy exchange should be the rate-limiting step. Also, in one of the simulations (at 1800 K) the vacancy exhibited several rotation steps before dissociating. This gives only one point in the Arrhenius plot, and no fitting can be performed. But since the activation energy of such a jump was calculated by TST, we can estimate the trial frequency from Eq. 2 by inserting the FPMD calculated frequency at the given temperature; $\nu^* = 3.8$ THz. Unfortunately, no solute-vacancy exchange was observed for Mn, except for unphysical jumps immediately after starting the simulations, probably originating from instabilities of the initial configuration. This means that we have failed to quantify the diffusivity of Mn using FPMD. Nevertheless, we have qualitatively established the rate limiting step, which means that the task of calculating the complete diffusivity from TST can be significantly simplified – only one set of vibrational frequencies needs to be calculated, not four.

Diffusion of Fe was quite similar to that of Mn, except that a large number of rotation jumps w_1 (NN1-NN1) took place (more than 130 out of the in total ~300 jumps recorded during the simulations) – consistent with a very low barrier for jumps (~20 kJ/mol). In addition to the rotations, dissociation of the solute-vacancy w_3 was quite frequent, both due to the weak repulsion and due to a relatively low diffusion barrier of ~60 kJ/mol. No exchange jumps were recorded in this case, which means that we can draw the same conclusion as in the case of Mn: The diffusivity should be calculated by TST, but only the w_2 jump frequency needs to be calculated, since the correlation factor is very close to 1.

3.3 Discussion

The three cases of Si, Mn, and Fe represent two typical situations in solute diffusion: rotation of the vacancy around the solute w_1 as the rate-limiting step (Si) and exchange of the solute and vacancy w_2 (Mn and Fe). They also constitute two different classes in that all the single jumps in Si diffusion exhibited low enough transition barriers to be probed by FPMD, while this was not the case for Mn and Fe. This means that FPMD could be used to quantify completely the diffusivity of Si in Al, while it could only give qualitative advice to TST calculations in the case of Mn and Fe. The gain from this observation is that the number of phonon calculations for jump frequency assessments could have been reduced from four to one in both cases. Mathematically, this corresponds to the correlation factor $f_2 = 1$.

This may seem as a small benefit from expensive calculations followed by detailed analyses. Also, one can object to the usefulness of the results by pointing to the obvious possibility to calculate the same transition barriers by TST. However, most of the analyses can be automated, so much of the information can be achieved with minimal investment of human resources.

The most important significance of this work is linked to how straightforward it is to employ similar FPMD calculations to more complicated systems with a large number of possible configurations and jumps; even to amorphous structures without well-defined sites. While we will not necessarily get out diffusivities from such FPMD simulations, we can hope that they will elucidate the rate-limiting mechanisms for diffusion, so that the task of calculating diffusivities from TST or related techniques can be considerably simplified. In some cases FPMD calculations

can even identify diffusion paths with lower barrier heights than the default ones originating from intuition or symmetry arguments.

As mentioned in the Methodology section, the simulation time needed to obtain even single jumps increases dramatically with the barrier height. The lowest single jump frequency in this work was that of solute-vacancy exchange in Mn, with $w_2 = 8.8\times10^7$ Hz at 1800 K. This implies that a simulation with time steps of 1 fs would need to run in the order of 10^7 steps per jump. A reasonable statistics may thus be feasible if the simulation time per time step is decreased significantly, either by reducing the cell size or by employing extra soft basis sets with a small number of plane waves per atom.[14] This relies on the superheating effect to sustain for such long simulation times, which is not obvious. When supercomputing resources and code efficiencies are developed further, it can be anticipated that all relevant jump barriers will become available at correct temperatures from FPMD with reasonable simulation cost.

4 Conclusions and outlook

Density functional theory calculations have been performed to assess the single jump frequencies and diffusion coefficients of Si, Fe, and Mn in Al using first principles molecular dynamics (FPMD) as well as first principles transition state calculations within the transition state theory (TST) formalism. Benchmark calculations using TST gave new values of the diffusivity of Si, Mn, and Fe. In particular, the contribution from the entropy of vacancy formation was revisited. It was possible to extract the complete diffusivity for Si from all levels of theory, and we found very good correspondence between the calculated diffusivity from FPMD and TST, with previous calculations and experimental results. The transition barrier of Mn and Fe exchange with the vacancy was too high for an appreciable statistics of jumps, and it was thus not possible to calculate the diffusivity directly from FPMD. However, the results could have been used to reduce the computational load of the TST significantly, since they clearly identified the rate-limiting step of the diffusion.

The most promising use of FPMD for solid state diffusion may thus be to clarify the most usual jump mechanisms in more complicated systems than that of single solutes diffusing in a perfect fcc lattice. This can be systems consisting of several interacting solutes, or solutes interacting with higher-dimensional defects like twins, stacking faults, or grain boundaries.

References

[1] J. B. Adams, S. M. Foiles, and W. G. Wolfer, J. Mater. Res. **4**, 102 (1989).

[2] N. Sandberg, B. Magyari-Kope, and T. R. Mattsson, Phys. Rev. Lett. **89**, 065901 (2002).

[3] P. E. Blochl, C. G. Vandewalle, and S. T. Pantelides, Phys. Rev. Lett. **64**, 1401 (1990).

[4] W. Frank, U. Breier, C. Elsasser, and M. Fahnle, Phys. Rev. Lett. **77**, 518 (1996).

[5] A. Janotti, M. Krcmar, C. L. Fu, and R. C. Reed, Phys. Rev. Lett. **92**, 085901 (2004).

[6] M. Krcmar, C. L. Fu, A. Janotti, and R. C. Reed, Acta Mater. **53**, 2369 (2005).

[7] V. Milman, M. C. Payne, V. Heine, R. J. Needs, J. S. Lin, and M. H. Lee, Phys. Rev. Lett. **70**, 2928 (1993).

[8] M. Mantina, Y. Wang, L. Q. Chen, Z. K. Liu, and C. Wolverton, Acta Mater. **57**, 4102 (2009).

[9] D. Simonovic and M. H. F. Sluiter, Phys. Rev. B **79**, 054304 (2009).

[10] G. H. Vineyard, J. Phys. Chem. Solids **3**, 121 (1957).

[11] G. Henkelman and H. Jonsson, J. Chem. Phys. **113**, 9978 (2000).

[12] G. Henkelman and H. Jonsson, J. Chem. Phys. **115**, 9657 (2001).

[13] A. F. Voter, F. Montalenti, and T. C. Germann, Annu. Rev. Mater. Sci. **32**, 321 (2002).

[14] E. Flage-Larsen, E. Sagvolden, O. M. Løvvik, and J. Friis, Subm. to J. Phys.: Condens. Matt. (2013).

[15] G. Kresse and J. Hafner, Phys. Rev. B **47**, 558 (1993).

[16] G. Kresse and J. Furthmuller, Phys. Rev. B **54**, 11169 (1996).

[17] J. P. Perdew and A. Zunger, Phys. Rev. B **23**, 5048 (1981).

[18] S. H. Vosko, L. Wilk, and M. Nusair, Can. J. Phys. **58**, 1200 (1980).

[19] P. Erhart, P. Jung, H. Schultz, and H. Ullmaier, in *Landolt-Bornstein* (Springer-Verlag, Berlin, 1991).

[20] R. W. Baluffi and P. S. Ho, in *Diffusion* (American Society for Metals, Metals Park, Ohio, USA, 1973).

[21] C. Wolverton, Acta Mater. **55**, 5867 (2007).

[22] G. H. Vineyard and G. J. Dienes, Phys. Rev. **93**, 265 (1954).

[23] K. Carling, G. Wahnstrom, T. R. Mattsson, A. E. Mattsson, N. Sandberg, and G. Grimvall, Phys. Rev. Lett. **85**, 3862 (2000).

[24] M. Mantina, Y. Wang, R. Arroyave, L. Q. Chen, Z. K. Liu, and C. Wolverton, Phys. Rev. Lett. **100**, 4, 215901 (2008).

[25] Y. Du *et al.*, Mater. Sci. Eng. A **363**, 140 (2003).

[26] W. B. Alexander and L. M. Slifkin, Phys. Rev. B **1**, 3274 (1970).

[27] G. M. Hood, Philos. Mag. **21**, 305 (1970).

[28] D. L. Beke, I. Godeny, I. A. Szabo, G. Erdelyi, and F. J. Kedves, Phil. Mag. A **55**, 425 (1987).

[29] C. Becker, G. Erdelyi, G. Hood, and H. Mehrer, in *Diffusion in Metals and Alloys, Pts 1-3: Dimeta 88*, edited by F. J. Kedves, and D. L. Beke1990), pp. 409.

[30] N. Sandberg and R. Holmestad, Phys. Rev. B **73**, 014108 (2006).

[31] N. L. Peterson and S. J. Rothman, Phys. Rev. B **1**, 3264 (1970).

[32] M. Mantina, S. L. Shang, Y. Wang, L. Q. Chen, and Z. K. Liu, Phys. Rev. B **80**, 184111 (2009).